BIOINFORMATICS ORIGINAL PAPER

Vol. 30 no. 11 2014, pages 1601–1608
doi:10.1093/bioinformatics/btu074

Structural bioinformatics

Advance Access publication February 3, 2014

The cleverSuite approach for protein characterization: predictions of structural properties, solubility, chaperone requirements and RNA-binding abilities

Petr Klus, Benedetta Bolognesi, Federico Agostini, Domenica Marchese, Andreas Zanzoni and Gian Gaetano Tartaglia*

Gene Function and Evolution, Centre for Genomic Regulation (CRG), Dr. Aiguader 88 and Universitat Pompeu Fabra (UPF), 08003 Barcelona, Spain

Associate Editor: Anna Tramontano

ABSTRACT

Motivation: The recent shift towards high-throughput screening is posing new challenges for the interpretation of experimental results. Here we propose the cleverSuite approach for large-scale characterization of protein groups.

Description: The central part of the cleverSuite is the cleverMachine (CM), an algorithm that performs statistics on protein sequences by comparing their physico-chemical propensities. The second element is called cleverClassifier and builds on top of the models generated by the CM to allow classification of new datasets.

Results: We applied the cleverSuite to predict secondary structure properties, solubility, chaperone requirements and RNA-binding abilities. Using cross-validation and independent datasets, the cleverSuite reproduces experimental findings with great accuracy and provides models that can be used for future investigations.

Availability: The intuitive interface for dataset exploration, analysis and prediction is available at http://s.tartaglialab.com/clever_suite.

Contact: gian.tartaglia@crg.es

Supplementary information: Supplementary data are available at *Bioinformatics* online.

Received on September 9, 2013; revised on January 17, 2014; accepted on February 20, 2014

1 INTRODUCTION

Due to the latest advances in technology, a large number of sequences have been deposited into databases (Harrow *et al.*, 2012; Wang *et al.*, 2012) and computational methods are being developed for their analysis and interpretation (Bailey *et al.*, 2009; Dinkel *et al.*, 2013). Some algorithms require per-case configuration (Buchan *et al.*, 2013) or lack intuitive interface (Rost, 1996), which prohibits diffusion among non-computational scientists.

Experimental scales encoding physico-chemical properties are useful to retrieve basic information on protein sequences (Wilkins *et al.*, 1999) and to predict features associated with protein folding (Gao *et al.*, 2010; Tartaglia and Vendruscolo, 2010), aggregation (Fernandez-Escamilla *et al.*, 2004; Tartaglia *et al.*, 2008) and molecular interactions (Cirillo *et al.*, 2013; Muppirala *et al.*, 2011). For instance, the Zyggregator method predicts aggregation propensity using a combination of physico-chemical properties including secondary structure, solvent accessibility, hydrophobicity and polarity (Tartaglia and Vendruscolo, 2008). Similarly, the SVMprot algorithm exploits amino acid properties to predict protein families annotated in Pfam (Cai *et al.*, 2003). Indeed, experimental scales can be employed to investigate large-scale properties of proteomes and identify common features (Hlevnjak *et al.*, 2012; Zanzoni *et al.*, 2013) but no systematic approach has been attempted so far to provide a general-purpose algorithm. We aim to provide researchers with an intuitive and statistically robust method to characterize protein groups exploiting the information contained in primary structure. Our premise is that the user should be able to make multiple hypotheses on the training sets and build models that others can test. As a general-purpose universal optimization is theoretically impossible (Ho and Pepyne, 2002), our strategy is to build a class of predictors that are specific for the individual problems. We pay particular attention to derive unbiased models because over-fitting of internal parameters can undermine the general applicability of algorithms (Hawkins, 2004; Tartaglia *et al.*, 2004).

Our approach, the cleverSuite, provides a series of easy-to-use, configuration-free tools with interactive graphical interface. The central part of the suite is the cleverMachine (CM), an algorithm to characterize protein datasets. CM does not require external fitting parameters and returns multiple physico-chemical properties ranked by their significance. Relevant properties are merged together to provide coherent and consistent classification, allowing complex feature analysis. The second element of our suite is the cleverClassifier (CC) that builds on top of results generated by the CM to allow classification of protein datasets using state of the art machine-learning approaches (Pedregosa *et al.*, 2011). CM and CC algorithms are freely available at http://s.tartaglialab.com/page/clever_suite.

We illustrate the powerfulness of our approach by making predictions of several protein features, including structural disorder (Sickmeier *et al.*, 2007), solubility (Niwa *et al.*, 2009), chaperone interactions (Calloni *et al.*, 2012; Kerner *et al.*, 2005) and RNA-binding abilities (Baltz *et al.*, 2012; Castello *et al.*, 2012). CM and CC models that are available for consultation at: http://s.tartaglialab.com/clever_community.

*To whom correspondence should be addressed.

2 METHODS

2.1 The cleverMachine

The algorithm evaluates relative difference in physico-chemical properties between two provided datasets. The first dataset is considered to be positive (P) and the second negative (N). The operations of the algorithm consist of multiple stages (Fig. 1).

2.1.1 Data generation The raw information is extracted from protein sequences using experimental physico-chemical propensities. Our curated database contains 80 physico-chemical propensities, derived from experimental data [e.g. hydrophobicity (Black and Mould, 1991; Bull and Breese, 1974; Fauchere and Pliska, 1983)] and statistics on computational tools. Physico-chemical propensities are organized into groups based on higher level properties (Fig. 2 and Supplementry Fig. S1). At present, we use eight classes (hydrophobicity, alpha-helix, beta-sheet, disorder, burial, aggregation, membrane and nucleic acid-binding propensities), but additional descriptors are allowed (see Section 2.3). For a given propensity, each protein sequence is scanned using a sliding window, moved one residue at a time, starting from the N-terminus (protein profile). The size of the sliding window is set to 7 amino acids to allow best discrimination between alpha helix (hydrogen bonding in the range $i+3 \rightarrow i$ and $i+5 \rightarrow i$) and beta sheet (strands between 3–10 amino acids) elements, but it can be modified.

2.1.2 Signal detection For each property, we count how many proteins from one dataset have profiles enriched with respect to the other dataset:

$$\text{coverage}\,(P, N) = \frac{1}{P_{\text{tot}}}\sum_{p} \vartheta\left(\frac{1}{N_{\text{tot}}}\sum_{n} \vartheta(\pi_p - \pi_n) - \alpha\right) \qquad (1)$$

In Equation (1), π is the signal extracted from the protein profile, the counter $\vartheta(x-y)$ is 1 if $x>y$ and 0 otherwise and P_{tot} and N_{tot} are the total number of sequences in P and N datasets. The internal parameter α is a cut-off used in the counting (see Section 2.1.6). The coverage is calculated for all proteins from both datasets and individual scale enrichments (i.e. fractions of P and N that can be discriminated) are calculated. For each physico-chemical propensity, the algorithm estimates the area under the receiver operating characteristics curve (AUC). In the five cases reported in this article, AUC and coverage(P, N) show more than 0.85 correlation (Fig. 3 and Supplementary Fig. S2). As AUC is cut-off independent, the high correlation indicates that coverage(P, N) depends only weakly on α. It is important to mention that the ROC analysis is not defined in multiple dimensions (Li and Fine, 2008), while different physico-chemical properties can be combined into an overall coverage. Coverage of 50% indicates that half of the dataset is differentially enriched (expectation for a random set is 25% corresponding to 0.5 of AUC; Fig. 3 and Supplementary Fig. S2).

2.1.3 Properties selection and combination To calculate the significance of each physico-chemical property, P and N are merged together and shuffled sets matching P and N in size are extracted. The procedure is repeated R times. For each of the randomized dataset pairs, we estimate the coverage. Information from the random dataset discrimination is used to rank properties significance using Z-scores and their associated P-values (Supplementary Fig. S3). Properties not meeting the criteria Z-score$>Z_{\text{th}}$

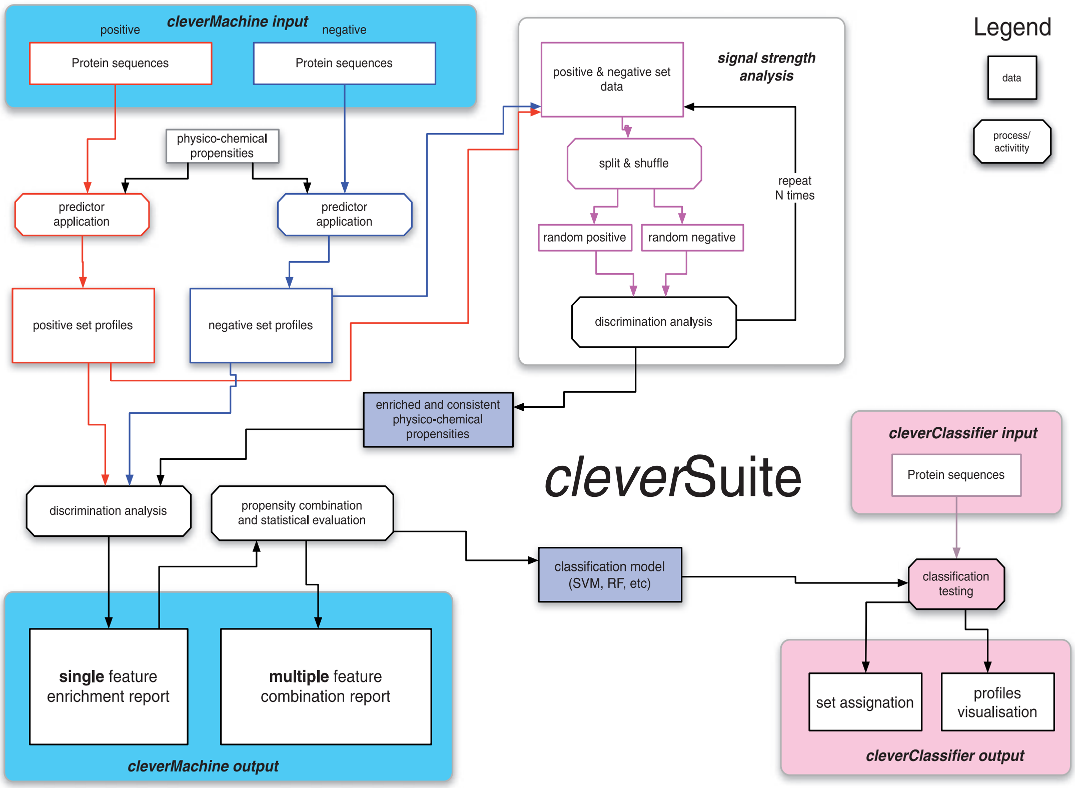

Fig. 1. The cleverSuite algorithm. The CM estimates the ability of physico-chemical properties to discriminate two input datasets. The statistical analysis gives information about individual property coverages and strength with respect to randomized sets. An exhaustive property-combination search is performed to assess the significance of the datasets separation. The CC uses the models generated by CM to classify new datasets to either the positive or negative set. Individual physico-chemical profiles are reported along with the discrimination statistics

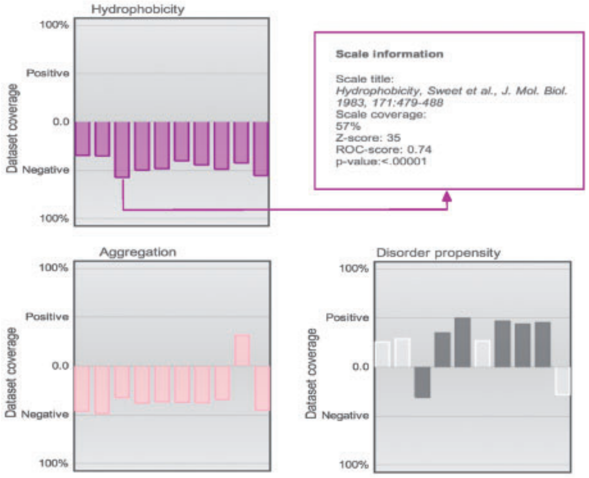

Fig. 2. Grouped property view. Example of properties grouped by class assignment and color (each property is described by 10 predictors). The *E.coli* solubility analysis is used as illustrative case: soluble proteins (positive case) are more disordered and less hydrophobic/aggregation prone. Low-significance properties (Z-score$<Z_{\mathrm{th}}$; $P > 0.01$; Section 2) are devoid of color. In the webserver, this view is interactive and shows information about each scale after clicking (see also Supplementary Fig. S1)

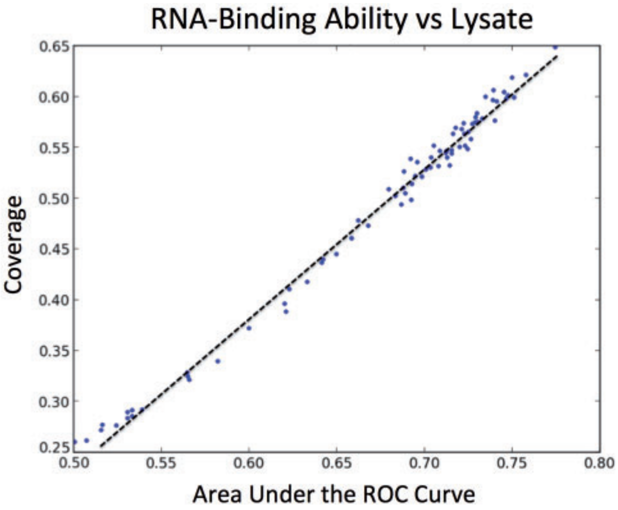

Fig. 3. Correlation between coverage and AUC. For the five cases presented in this study, AUC and coverage of individual physico-chemical properties show a correlation $r>0.85$. In this example, we use human RNA-binding proteins (compared with lysate; $r=0.95$)

and P-value<0.01 are excluded from the analysis. Using 500 random sets, we observe that optimal values are $Z_{\mathrm{th}}=6$ and $R=15$. To check consistencies among predictors of the same physico-chemical propensity, we group the properties by higher level features and also highlight the ones that pass the selection criteria (Fig. 2 and Supplementary Fig. S1). For each combination of properties ranging from 1 to 5 ($\sim 10^7$ alternatives), the overall coverage (union of individual coverages) is calculated and the best-performing set is selected (Fig. 4). We observe that some physico-chemical properties are correlated. Nevertheless, since the algorithm selects only the most discriminative combination of properties, correlation does not represent a limitation. In fact, if two properties produce overlapping lists of proteins, their combination creates smaller coverage compared to scales that are more different.

2.1.4 Model generation In order to identify the best model for further set classification, the algorithm evaluates combination of scales with multiple machine learning methodologies. The selected classifiers include random forests, support vector machine, nearest neighbour and adaptive boosting algorithms (Pedregosa *et al.*, 2011). To avoid set size bias, we perform multiple equal size samplings from each of the datasets. Moreover, we perform 10-fold cross-validation with each of the models to select the best performing (highest accuracy) algorithm.

2.2 The cleverClassifier

The main goal is the set-wide assignment of query X to either P or N set from the reference submission (Fig. 1). The prediction is carried out using the best model evaluated on reference data. CD-HIT (Fu *et al.*, 2012) algorithm is employed to detect set sequence similarity of X with respect to reference. If the similarity exceeds 10%, the value is reported to the user. Random sets generated with the same AA composition as the reference sets are employed to estimate signal strength, which is defined as the difference between performance of set X (i.e. fraction of cases that can be classified) and random sets. Signal strength ranges between 0 (no enrichment) to 0.5 (strong signal) (Supplementary Tables S1 and S2). For each of the entries from dataset X, individual physico-chemical profiles (Supplementary Fig. S4) are reported together with element assignment to either P or N. Moreover, for each individual prediction we estimate prediction strength using consensus from cross-validation models.

2.3 Additional features

(i) *Custom scales*: if the 'expert mode' option is selected in the webserver, the user can submit up to 10 amino acid scales for CM calculations. As CM employs 10 scales for each physico-chemical group (e.g. hydrophobicity) we suggest a similar approach for the choice of additional scales. Custom scales do not need to be normalized.

(ii) *Derived scale*: at every run, CM produces an *ad hoc* scale derived from the input sets ('expert mode'). The scale is measured by considering the frequency of each amino acid a in both sets P and N:

$$\Delta f(a) = f_P(a) - f_N(a) \tag{2}$$

In Equation (2), amino acid frequencies are normalized: $\sum_a f_P(a) = \sum_a f_N(a) = 1$. The derived scale can be used in CC runs (see (i) above).

(iii) *Adaptive threshold*: the optimal cut-off α corresponds to the highest coverage with respect to shuffled sets:

$$\alpha : \max\left[\mathrm{coverage}(P, N) - \frac{1}{R}\sum_r \mathrm{coverage}(P_r, N_r)\right] \tag{3}$$

The number of shuffled sets P_r and N_r is $R = 15$. If the 'expert mode' option is selected, the algorithm optimizes α for the input sets. In the 'normal run' mode, the cut-off is $\alpha = 0.75$ (Supplementary Fig. S5).

(iv) *Peak detection*: the coverage can be computed using (a) the average of physico-chemical profiles or (b) regions that deviate more than one standard deviation from the average score. Average score and standard deviation are estimated from the distribution of profiles (considering both positive and negative sets). The use of a threshold, previously implemented for the calculation of aggregation properties (Tartaglia and Vendruscolo, 2008), introduces a sequence-position dependency in the calculation of profiles.

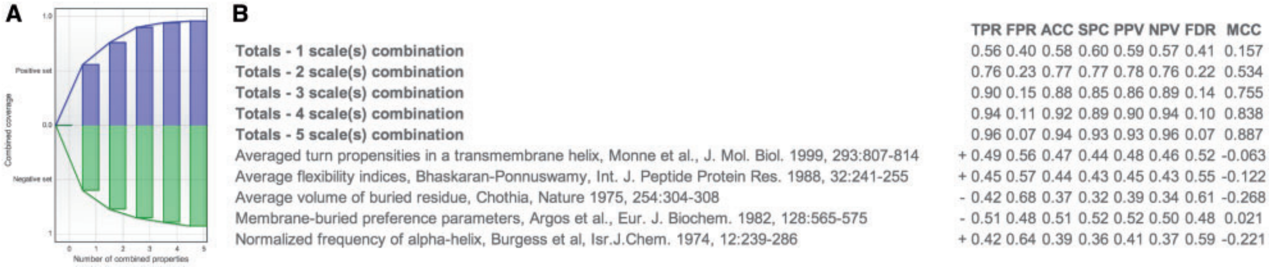

		TPR	FPR	ACC	SPC	PPV	NPV	FDR	MCC
Totals - 1 scale(s) combination		0.56	0.40	0.58	0.60	0.59	0.57	0.41	0.157
Totals - 2 scale(s) combination		0.76	0.23	0.77	0.77	0.78	0.76	0.22	0.534
Totals - 3 scale(s) combination		0.90	0.15	0.88	0.85	0.86	0.89	0.14	0.755
Totals - 4 scale(s) combination		0.94	0.11	0.92	0.89	0.90	0.94	0.10	0.838
Totals - 5 scale(s) combination		0.96	0.07	0.94	0.93	0.93	0.96	0.07	0.887
Averaged turn propensities in a transmembrane helix, Monne et al., J. Mol. Biol. 1999, 293:807-814	+	0.49	0.56	0.47	0.44	0.48	0.46	0.52	-0.063
Average flexibility indices, Bhaskaran-Ponnuswamy, Int. J. Peptide Protein Res. 1988, 32:241-255	+	0.45	0.57	0.44	0.43	0.45	0.43	0.55	-0.122
Average volume of buried residue, Chothia, Nature 1975, 254:304-308	-	0.42	0.68	0.37	0.32	0.39	0.34	0.61	-0.268
Membrane-buried preference parameters, Argos et al., Eur. J. Biochem. 1982, 128:565-575	-	0.51	0.48	0.51	0.52	0.52	0.50	0.48	0.021
Normalized frequency of alpha-helix, Burgess et al, Isr.J.Chem. 1974, 12:239-286	+	0.42	0.64	0.39	0.36	0.41	0.37	0.59	-0.221

Fig. 4. Scale combinations and statistics. (A) Relationship between the number of combined scales and the coverages for both positive (blue bars) and negative (green bars) datasets. (B) Statistics for each scale combination and its individual members. In the webserver, click-through the combination titles reveals scales contained and detailed statistics (three-scale combination is shown; the *E.coli* solubility analysis is used as example). This view is used to summarize results of both CM and CC

3 RESULTS

A sketch describing CM and CC workflow is presented in Figure 1. The goal of the CM algorithm is to discriminate between two protein sets. A number of properties, including hydrophobicity, alpha-helical, beta-sheet, disorder, burial, aggregation, membrane and nucleic acid-binding propensities, are employed to build physicochemical 'profiles'. The physico-chemical properties are combined together to identify similarities and differences between the two sets. Once the discriminating properties are characterized, CM generates a model, which is employed by CC to classify new datasets. As shown in the examples below, we tested CM and CC performances on protein features such as secondary structure, structural disorder, solubility, chaperone requirements and RNA-binding ability (Supplementary Table S1). Unless otherwise stated, we always remove overlap between training and test sets using CD-HIT with default cut-off set for sequence similarity (Fu *et al.*, 2012).

Table 1. cleverSuite performances

	cleverSuite			Reference		
	ACC[a] (%)	TPR[b] (%)	TNR[b] (%)	Method	TPR[c] (%)	TNR[c] (%)
Alpha-beta	97.9	90.4	93.2	RePROF	92.6	72.0
Disorder	86.1	84.5	73.6	FoldIndex	62.9	64.7
Solubility	89.8	84.7	60.5	PROSO II	78.5	74.0
Chaperones	81.6	75.4	60.0	Limbo	100.0	22.5
mRNA	84.3	72.9	79.2	RNApred	82.5	52.8

[a] A 10-fold cross-validation accuracy for CM models (ACC is accuracy).
[b] Independent validation performances for CC.
[c] Performance comparison with algorithms reported in literature. TPR (true positive rate) and TNR (true negative rate) are calculated on the same sets used to validate CC. Links to full results are given in Supplementary Table S1.

3.1 Alpha-helix versus beta-sheet proteins

In this first introductory example, we trained CM to distinguish between alpha-helical and beta-sheet proteins. The PDB database (Bernstein *et al.*, 1977) was used to retrieve protein structures, STRIDE (Heinig and Frishman, 2004) was applied to analyse alpha-helical and beta-sheet content and CD-HIT (Fu *et al.*, 2012) was employed to filter out sequences with >50% identity. After sequence redundancy removal, the alpha-helical set consisted of 277 proteins adopting >80% of alpha-helical conformation while the beta-sheet set was comprised of 191 proteins containing >60% of beta-sheet content. Sequences coding for alpha-helical structures were used to build the positive set, while the negative set consisted of beta-sheet proteins.

3.1.1 Performances In striking agreement with structural classification, we found that even a single physico-chemical scale of alpha-helical propensity (Deléage and Roux, 1987) is able to discriminate 98% of the two sets with a 99.0% accuracy and 100% precision (Table 1). Hence, CM shows ideal performances in separating alpha-helical and beta-sheet proteins. All alpha-helical scales (Burgess *et al.*, 1974; Chou and Fasman, 1978; Kanehisa and Tsong, 1980) showed consistent enrichment in the positive set, while the beta propensity scales displayed significant enrichment in the negative set (the signal is strong with respect to permutated input sets with P-value < 0.01) (Chou and Fasman, 1978; Deléage and Roux; Kanehisa and Tsong, 1980; Levitt, 1978; Prabhakaran, 1990).

3.1.2 Cross-validation Through a 10-fold cross-validation on both sets, our CM showed accuracy of 97.9% (Table 1). When compared to random sets, the signal strength was 0.5 (Supplementary Table S2). CM selected AdaBoost (Pedregosa *et al.*, 2011) classifier as the best performing algorithm for this calculation.

3.1.3 Independent validations We downloaded alpha/beta proteins from SCOP (Andreeva *et al.*, 2008). After redundancy removal (CD-HIT 50), the alpha-helical set consisted of 176 proteins adopting >80% of alpha-helical conformation while the beta-sheet set was comprised of 79 proteins containing >60% of beta-sheet content. Our predictions showed accuracy of 90.4% for alpha-helical (positive set) and 93.2% for beta-sheet (negative set) assignments (Table 1). The testing sets achieved separation from random of 0.4 (alpha-helix) and 0.4 (beta-sheet). On the same datasets, the RePROF (Rost, 1996) algorithm yielded accuracies of 92.6% (alpha-helical proteins) and 72.1% (beta-sheet proteins; Table 1 and Supplementary Material). As an additional test we used NetSurfP (Petersen *et al.*, 2009) that achieved accuracy of 96% (alpha-helical proteins) and 64% (beta-sheet proteins).

3.2 Structural disorder

It has been shown that natively unfolded proteins are implicated in cellular regulation, signalling and assembly of macromolecular complexes (Dunker *et al.*, 2002). Absence of native structure has functional implications for complex organisms (Koonin *et al.*, 2002). In fact, higher eukaryotes show larger amount of intrinsically disordered proteins with respect to prokaryotes (Tartaglia *et al.*, 2005). We applied our algorithm to intrinsically disordered proteins [positive set containing 630 proteins from DisProt (Sickmeier *et al.*, 2007)] and structured proteins [negative set containing 3347 proteins from SCOP (Andreeva *et al.*, 2008)].

3.2.1 Performances CM identifies disorder as the most discriminative physico-chemical property: TOP-IDB and DisProt cover respectively 65.5% and 61.0% (Campen *et al.*, 2008; Sickmeier *et al.*, 2007). We found that disordered proteins are more hydrophilic and soluble. Indeed, the coverage is 50% for hydrophobicity [corresponding to 0.7 of AUC (Eisenberg *et al.*, 1984)], 45% for aggregation (Tartaglia and Vendruscolo, 2010) and 42% for burial (Harpaz *et al.*, 1994). The CM achieves optimal performances by combining the scales for disorder (Sickmeier *et al.*, 2007), hydrophobicity (Eisenberg *et al.*, 1984), burial (Harpaz *et al.*, 1994), aggregation (Tartaglia and Vendruscolo, 2010) and alpha-helix (Kanehisa and Tsong, 1980) (sensitivity of 0.9 and false positive rate of 0.07).

3.2.2 Cross-validation Through a 10-fold cross-validation on both sets, our CM showed accuracy of 86.7% (Table 1). When compared to random sets, the signal strength was 0.4 (Supplementary Table S2). The best performing classifier for this case was Extremely Randomized Trees (Pedregosa *et al.*, 2011), a variant of the Random Forest ensemble classifier.

3.2.3 Independent validations As a positive set we used a database of yeast prions that are enriched in structural disorder [27 entries after sequence redundancy removal (Alberti *et al.*, 2009)]. The negative set was comprised of a manually curated database of structured proteins whose folded native state has been studied *in vitro* [44 entries after sequence redundancy removal (Tartaglia and Vendruscolo, 2010)]. Our predictions showed accuracy of 84.5% for prions and 73.6% for structured proteins (Table 1). The testing sets achieved separation from random of 0.4 (prions) and 0.2 (structured proteins). On the same datasets, the FoldIndex (Prilusky *et al.*, 2005) algorithm yielded accuracies of 62.9% (prions) and 64.7% (structured proteins; Table 1 and Supplementary Material). In addition, we employed NetSurfP (Petersen *et al.*, 2009) and observed accuracies of 88.8% (prions) and 63.7% (structured proteins).

3.3 Solubility

A number of proteins such as fragile X mental retardation protein FMRP, TAR–DNA-binding protein 43 TDP43, fused in sarcoma FUS and prions have a strong propensity to aggregate into amyloid fibrils (Cirillo *et al.*, 2013). Hence, prediction of protein solubility is fundamental to understand functional (e.g. RNA-binding) and dysfunctional (e.g. aggregated) states. To build a predictor of protein solubility, we took advantage of a study in which the solubility of 70% of *Escherichia coli* proteins was experimentally measured using an *in vivo* translation system (Niwa *et al.*, 2009). In this analysis, we ranked proteins by their solubility and used top (1000 soluble proteins) and bottom (1000 insoluble proteins) elements as the positive and negative sets (Agostini *et al.*, 2012).

3.3.1 Performances In agreement with experimental evidence (Niwa *et al.*, 2009), we found that hydrophobicity (Fauchere and Pliska, 1983; Sweet and Eisenberg, 1983) (coverage of 54–57%), aggregation (Conchillo-Solé *et al.*, 2007) (coverage of 49%) and burial (Wertz and Scheraga, 1978) (coverage of 58%) propensities are depleted in the positive set while disorder (Campen *et al.*, 2008) (coverage of 50%) and alpha-helix (Kanehisa and Tsong, 1980) (coverage of 41%) propensities are enriched (Fig. 2 and Supplementary Fig. S2). By selecting the scales for disorder (Bhaskaran and Ponnuswamy, 1988; Monné *et al.*, 1999), burial (Argos *et al.*, 1982; Chothia, 1975) and alpha-helix (Burgess *et al.*, 1974) the algorithm reported optimal performances associated with sensitivity of 0.96 and false positive rate of 0.07 (Fig. 4).

3.3.2 Cross-validation Through a 10-fold cross-validation on both sets, our CM showed accuracy of 89.7% (Table 1). When compared to random sets, the signal strength was 0.5 (Supplementary Table S2). In this case, Random Forest classifier (Pedregosa *et al.*, 2011) was selected as the best performing.

3.3.3 Independent validations As positive set we used proteins whose folding kinetics and thermodynamics have been studied *in vitro* [71 non-redundant entries (Tartaglia and Vendruscolo, 2010)]. The negative set contained proteins requiring molecular chaperones to fold into native structure [81 entries (Kerner *et al.*, 2005)]. Our predictions showed accuracy of 84.7% for the positive set and 60.5% for the negative. The testing achieved separation from random of 0.5 (soluble proteins) and 0.1 (insoluble proteins). On the same datasets, PROSO II (Smialowski *et al.*, 2012) algorithm yielded accuracies of 78.5% (positive set) and 74% (negative set; Table 1; Supplementary Material).

3.4 Chaperone requirements

Hsp70, the major stress-induced heat shock protein, facilitates substrate folding into native state (Calloni *et al.*, 2012; Hartl and Hayer-Hartl, 2002) and is able to associate with AU-rich transcripts (Kishor *et al.*, 2013; Zimmer *et al.*, 2001). Mass spectrometry experiments show that *E.coli* DnaK interacts with proteins lacking strong hydrophobic core or exposing regions that are buried in the native state. In our analysis, the positive set was composed of proteins that require DnaK/GroEL to fold properly (109 sequences) and the negative set consisted of independently folding proteins [39 sequences (Kerner *et al.*, 2005)].

3.4.1 Performances Our results show strong agreement with experimental findings, with proteins in the positive set having low hydrophobic propensity [43% coverage (Eisenberg *et al.*, 1984)] but high burial propensity [68% coverage (Rose *et al.*, 1985)], which is consistent with the observation that lack of a hydrophobic core prevents from folding into native state (Tartaglia *et al.*, 2010). In agreement with experimental evidence (Zimmer *et al.*, 2001), we found that the positive set is enriched in proteins binding to nucleic acids (Zimmer *et al.*, 2001; Calloni *et al.*, 2012; Kishor *et al.*, 2013). By automatically combining the scales for nucleic acid binding (Lewis *et al*., 2011), burial (Argos *et al*., 1982; Rose *et al*., 1985), membrane (Argos *et al*., 1982) and hydrophobicity (Eisenberg *et al*., 1984) propensities, CM achieved a sensitivity of 0.91 and false positive rate of 0.08.

3.4.2 Cross-validation Through a 10-fold cross-validation we find that CM has accuracy of 81.6% and separation from random of 0.3 (Table 1 and Supplementary Table S2). The best performance was achieved with the AdaBoost (Pedregosa *et al*., 2011) classification algorithm.

3.4.3 Independent validations The positive validation set was comprised of proteins requiring chaperones to fold (81 entries) (Kerner *et al*., 2005) while the negative validation was a manually curated dataset of independently-folding proteins [71 non-redundant entries (Tartaglia and Vendruscolo, 2010)]. The independent sets achieved accuracies of 75.4% for chaperone-dependent set and 60% for independently folding proteins. The testing sets achieved separations from random of 0.2 (chaperone-dependent and -independent set). To compare our performance to existing methods, we used Limbo (Van Durme *et al*., 2009) to predict DnaK-binding affinity of protein peptides. The method classified 100% of the positive set as chaperone-dependent (the accuracy was 96% on the positive training set), and it achieved 22.5% assignation accuracy on the independently folding dataset (Table 1 and Supplementary Material).

3.5 RNA-binding abilities

Recent technological advances have made it possible to discover that number of proteins have RNA-binding ability (Riley and Steitz, 2013). We focused on RNA-interacting proteins (715 entries) detected with UV cCL and PAR-CL protocols on proliferating HeLa cells and compared them with the cell lysate [2831 entries after sequence redundancy removal (Castello *et al*., 2012)].

3.5.1 Performances The single property analysis revealed a strong and consistent RNA-binding property of the dataset: RNA-binding scales (Castello *et al*., 2012; Lewis *et al*., 2011; Terribilini *et al*., 2006) cover between 62–65%. Moreover, it has been observed that protein disorder is an important feature for RNA-binding proteins (Bellay *et al*., 2011; Cirillo *et al*., 2014). In agreement with this result, we found a significant enrichment in disorder propensities (Bhaskaran and Ponnuswamy, 1988; Campen *et al*., 2008). CM automatically selects the scales for RNA binding (Castello *et al*., 2012; Lewis *et al*., 2011), disorder (Campen *et al*., 2008; Isogai *et al*., 1980) and aggregation propensities (Tartaglia *et al*., 2008) achieving a sensitivity of 0.91 and false positive rate of 0.07 on the entire dataset.

3.5.2 Cross-validation A 10-fold cross-validation on both datasets yielded accuracy of 84.3% and separation from random of 0.5 (Table 1 and Supplementary Table S2). The Extremely Randomised Tree classifier (Pedregosa *et al*., 2011) was selected as the best performing algorithm for this case.

3.5.3 Independent validations The positive set contained proteins identified as RNA-binding using quantitative proteomics (Baltz *et al*., 2012). We removed any overlap between training and test sets using CD-HIT (Fu *et al*., 2012), leaving the positive set size to 86 entries. The negative validation contained 250 not nucleic acid binding proteins (Shazman and Mandel-Gutfreund, 2008). Our predictions showed accuracy of 72.9% for the mRNA-binding set and 79.2% for the negative validation. The separation from internal random dataset was respectively 0.5 and 0.1 for the positive and negative testing sets. Using the same data as for CC validation, the RNApred (Kumar *et al*., 2011) achieved accuracy of 82.5% for the positive set and 52.8% for the negative validation (Table 1; Supplementary Material).

4 DISCUSSION

The cleverSuite provides a novel and unique approach for both characterization and classification of protein groups. In striking agreement with experimental evidence, we reported accurate predictions of protein solubility in *E.coli* (Niwa *et al*., 2009), RNA-binding ability in *H. Sapiens* (Castello *et al*., 2012), structural disorder (Sickmeier *et al*., 2007) and chaperone requirements (Kerner *et al*., 2005). Our performances are comparable to other algorithms that were built to predict specific protein features. In agreement with previous observations, we found that physicochemical propensities linked to structural disorder and are relevant for RNA-binding, chaperone requirement and solubility (Agostini *et al*., 2012; Calloni *et al*., 2012; Cirillo *et al*., 2014), which very well captures the central role of natively unfolded proteins in higher eukaryotes (Babu *et al*., 2011). This observation is further supported by direct comparison of *H.sapiens* and *E.coli* proteomes, which shows enrichment in hydrophobicity and aggregation propensity for *E.coli* and structural disorder for *H.sapiens* (all links to results are provided in Supplementary Table S1).

Our findings suggest that the cleverSuite is an ideal tool to analyse the outcome of large-scale experiments. As shown in the examples, the algorithm can be applied to very diverse types of cases to allow a fine classification of protein features (Table 1). Future plans include incorporation of more properties and alternative ways to extract the signal from protein profiles. At present, the choice of propensity scales is mainly based on their previous use but custom scales are allowed in the webserver. We would like to note that our approach is not restricted to propensity scales and that any function mapping a primary structure into a profile could be interfaced with the algorithm. In next version, we are planning to implement the projection of profiles onto orthonormal bases, which should improve our performances.

In the CM each physico-chemical property is described by same number of propensity scales (eight groups containing 10 scales each; Fig. 2 and Supplementary Fig. S3), which guarantees that there is not over-representation of a particular property. We stress that the algorithm is built in a way that only non-correlated scales are selected for the analysis. In fact, if two scales discriminate the same set of proteins, their combination together would result in a smaller coverage compared to non-correlated scales. The CM can compute up to 10 millions associations of propensities (i.e. five scales out of 80 groups) to find the optimal combination, which is computationally expensive but ensures an impartial and exhaustive search. For this reason, the calculations have been parallelized to complete the analysis in short time, even when the input sets are large. We could have used other algorithms instead of the exhaustive search, but our focus is the simple and clear interpretation of scale contributions, which is not possible through more complex approaches.

We base our approach on the assumption that the algorithm works optimally if the system is able to select its predictors without external intervention (Wolpert, 2002). Similarly to what has been done to rationalize the determinants of protein aggregation (Chiti *et al.*, 2003), the cleverSuite identifies the most relevant properties for a specific problem with the main differences being that: (i) fitting parameters are avoided and (ii) features are selected from a large pool of physico-chemical characteristics. Notably, the method allows the user to choose the reference set, which is strategic to circumvent the problem of the lack of negative cases in literature (Smialowski *et al.*, 2010).

Although other useful tools are available to analyse protein features (Hall *et al.*, 2009; Rao *et al.*, 2011), we did not find any general-purpose method to discriminate datasets using parameter-free combinations of physico-chemical characteristics and we hope that our efforts will inspire future studies in the field. In conclusion, the cleverSuites offers an easy-to-use interface, accessible to a wide range of experimental and computational scientists.

Submissions are by default private, however, if a user wishes to share an analysis result or a classifier, there is an option to publish links on the 'featured results' page (http://s.tartaglialab.com/clever_community, maintained by the authors).

ACKNOWLEDGEMENTS

We thank Ben Lehner, Gianni de Fabritiis and Roderic Guigo' for their advice on this work.

Funding: This work was supported by Spanish Ministry of Economy and Competitiveness (SAF2011-26211); European Research Council (ERC Starting Grant RYBOMYLOME to G.G.T.); 'la Caixa' (grant to P.K.). Marie Curie Action (to B.B.).

Conflict of interest: none declared.

REFERENCES

Agostini,F. *et al.* (2012) Sequence-based prediction of protein solubility. *J. Mol. Biol.*, **421**, 237–241.

Alberti,S. *et al.* (2009) A systematic survey identifies prions and illuminates sequence features of prionogenic proteins. *Cell*, **137**, 146–158.

Andreeva,A. *et al.* (2008) Data growth and its impact on the SCOP database: new developments. *Nucleic Acids Res.*, **36**, D419–D425.

Argos,P. *et al.* (1982) Structural prediction of membrane-bound proteins. *Eur. J. Biochem.*, **128**, 565–575.

Babu,M.M. *et al.* (2011) Intrinsically disordered proteins: regulation and disease. *Curr. Opin. Struct. Biol.*, **21**, 432–440.

Bailey,T.L. *et al.* (2009) MEME Suite: tools for motif discovery and searching. *Nucleic Acids Res.*, **37**, W202–W208.

Baltz,A.G. *et al.* (2012) The mRNA-bound proteome and its global occupancy profile on protein-coding transcripts. *Mol. Cell*, **46**, 674–690.

Bellay,J. *et al.* (2011) Bringing order to protein disorder through comparative genomics and genetic interactions. *Genome Biol.*, **12**, R14.

Bernstein,F.C. *et al.* (1977) The Protein Data Bank: a computer-based archival file for macromolecular structures. *J. Mol. Biol.*, **112**, 535–542.

Bhaskaran,R. and Ponnuswamy,P.k. (1988) Positional flexibilities of amino acid residues in globular proteins. *Int. J. Peptide Protein Res.*, **32**, 241–255.

Black,S.D. and Mould,D.R. (1991) Development of hydrophobicity parameters to analyze proteins which bear post- or cotranslational modifications. *Anal. Biochem.*, **193**, 72–82.

Buchan,D.W.A. *et al.* (2013) Scalable web services for the PSIPRED protein analysis workbench. *Nucleic Acids Res.*, **41**, W349–W357.

Bull,H.B. and Breese,K. (1974) Surface tension of amino acid solutions: a hydrophobicity scale of the amino acid residues. *Arch. Biochem. Biophys*, **161**, 665–670.

Burgess,A. *et al.* (1974) Analysis of conformation of amino acid residues and prediction of backbone topography in proteins. *Isr. J. Chem.*, 239–286.

Cai,C.Z. *et al.* (2003) SVM-Prot: web-based support vector machine software for functional classification of a protein from its primary sequence. *Nucleic Acids Res.*, **31**, 3692–3697.

Calloni,G. *et al.* (2012) DnaK functions as a central hub in the *E.coli* chaperone network. *Cell Reports*, **1**, 251–264.

Campen,A. *et al.* (2008) TOP-IDP-scale: a new amino acid scale measuring propensity for intrinsic disorder. *Protein Pept. Lett.*, **15**, 956–63.

Castello,A. *et al.* (2012) Insights into RNA biology from an atlas of mammalian mRNA-binding proteins. *Cell*, **149**, 1393–1406.

Chiti,F. *et al.* (2003) Rationalization of the effects of mutations on peptide and protein aggregation rates. *Nature*, **424**, 805–808.

Chothia,C. (1975) Structural invariants in protein folding. *Nature*, **254**, 304–308.

Chou,P.Y. and Fasman,G.D. (1978) Prediction of the secondary structure of proteins from their amino acid sequence. *Adv. Enzymol. Relat. Areas Mol. Biol.*, **47**, 45–148.

Cirillo,D. *et al.* (2014) Constitutive patterns of gene expression regulated by RNA-binding proteins. *Genome Biol.*, **15**, R13.

Cirillo,D. *et al.* (2013) Neurodegenerative diseases: quantitative predictions of protein-RNA interactions. *RNA*, **19**, 129–140.

Conchillo-Solé,O. *et al.* (2007) AGGRESCAN: a server for the prediction and evaluation of 'hot spots' of aggregation in polypeptides. *BMC Bioinform.*, **8**, 65.

Deléage,G. and Roux,B. (1987) An algorithm for protein secondary structure prediction based on class prediction. *Protein Eng.*, **1**, 289–294.

Dinkel,H. *et al.* (2013) The eukaryotic linear motif resource ELM: 10 years and counting. *Nucleic Acids Res.*, **42**, D259–D266

Dunker,A.K. *et al.* (2002) Intrinsic disorder and protein function. *Biochemistry*, **41**, 6573–6582.

Van Durme,J. *et al.* (2009) Accurate prediction of DnaK-peptide binding via homology modelling and experimental data. *PLoS Comput. Biol.*, **5**, e1000475.

Eisenberg,D. *et al.* (1984) Analysis of membrane and surface protein sequences with the hydrophobic moment plot. *J. Mol. Biol.*, **179**, 125–142.

Fauchere,J. and Pliska,V. (1983) Hydrophobic parameters pi of amino-acid side chains from the partitioning of N-acetyl-amino-acid amides. *Eur. J. Med. Chem.*, **18**, 369–375.

Fernandez-Escamilla,A.-M. *et al.* (2004) Prediction of sequence-dependent and mutational effects on the aggregation of peptides and proteins. *Nat. Biotechnol.*, **22**, 1302–1306.

Fu,L. *et al.* (2012) CD-HIT: accelerated for clustering the next-generation sequencing data. *Bioinformatics*, **28**, 3150–3152.

Gao,J. *et al.* (2010) Accurate prediction of protein folding rates from sequence and sequence-derived residue flexibility and solvent accessibility. *Proteins*, **78**, 2114–2130.

Hall,M. *et al.* (2009) The WEKA Data Mining Software: An Update. *SIGKDD Explor. Newsl.*, **11**, 10–18.

Harpaz,Y. *et al.* (1994) Volume changes on protein folding. *Structure*, **2**, 641–649.

Harrow,J. *et al.* (2012) GENCODE: the reference human genome annotation for The ENCODE Project. *Genome Res.*, **22**, 1760–1774.

Hartl,F.U. and Hayer-Hartl,M. (2002) Molecular chaperones in the cytosol: from nascent chain to folded protein. *Science*, **295**, 1852–1858.

Hawkins,D.M. (2004) The problem of overfitting. *J. Chem. Inf. Comput. Sci.*, **44**, 1–12.

Heinig,M. and Frishman,D. (2004) STRIDE: a web server for secondary structure assignment from known atomic coordinates of proteins. *Nucleic Acids Res.*, **32**, W500–W502.

Hlevnjak,M. *et al.* (2012) Sequence signatures of direct complementarity between mRNAs and cognate proteins on multiple levels. *Nucleic Acids Res.*, **40**, 8874–8882.

Ho,Y.C. and Pepyne,D.L. (2002) Simple explanation of the no-free-lunch theorem and its implications. *J. Optim. Theor. Appl.*, **115**, 549–570.

Isogai,Y. *et al.* (1980) Characterization of multiple bends in proteins. *Biopolymers*, **19**, 1183–1210.

Kanehisa,M.I. and Tsong,T.Y. (1980) Local hydrophobicity stabilizes secondary structures in proteins. *Biopolymers*, **19**, 1617–1628.

Kerner,M.J. *et al.* (2005) Proteome-wide analysis of chaperonin-dependent protein folding in *Escherichia coli*. *Cell*, **122**, 209–20.

Kishor,A. *et al.* (2013) Hsp70 is a novel posttranscriptional regulator of gene expression that binds and stabilizes selected mRNAs containing AU-rich elements. *Mol. Cell Biol.*, **33**, 71–84.

Koonin,E.V. *et al.* (2002) The structure of the protein universe and genome evolution. *Nature*, **420**, 218–223.

Kumar,M. *et al.* (2011) SVM based prediction of RNA-binding proteins using binding residues and evolutionary information. *J. Mol. Recognit.*, **24**, 303–313.

Levitt,M. (1978) Conformational preferences of amino acids in globular proteins. *Biochemistry*, **17**, 4277–4285.

Lewis,B.A. *et al.* (2011) PRIDB: a protein–RNA interface database. *Nucleic Acids Res.*, **39**, D277–D282.

Li,J. and Fine,J.P. (2008) ROC analysis with multiple classes and multiple tests: methodology and its application in microarray studies. *Biostatistics*, **9**, 566–576.

Monné,M. *et al.* (1999) Turns in transmembrane helices: determination of the minimal length of a 'helical hairpin' and derivation of a fine-grained turn propensity scale. *J. Mol. Biol.*, **293**, 807–814.

Muppirala,U.K. *et al.* (2011) Predicting RNA-protein interactions using only sequence information. *BMC Bioinformatics*, **12**, 489.

Niwa,T. *et al.* (2009) Bimodal protein solubility distribution revealed by an aggregation analysis of the entire ensemble of Escherichia coli proteins. *Proc. Natl Acad. Sci. USA*, **106**, 4201–4206.

Pedregosa,F. *et al.* (2011) Scikit-learn: machine learning in python. *J. Mach. Learn. Res.*, **12**, 2825–2830.

Petersen,B. *et al.* (2009) A generic method for assignment of reliability scores applied to solvent accessibility predictions. *BMC Struct. Biol.*, **9**, 51.

Prabhakaran,M. (1990) The distribution of physical, chemical and conformational properties in signal and nascent peptides. *Biochem. J.*, **269**, 691–696.

Prilusky,J. *et al.* (2005) FoldIndex©: a simple tool to predict whether a given protein sequence is intrinsically unfolded. *Bioinformatics*, **21**, 3435–3438.

Rao,H.B. *et al.* (2011) Update of PROFEAT: a web server for computing structural and physicochemical features of proteins and peptides from amino acid sequence. *Nucleic Acids Res.*, **39**, W385–W390.

Riley,K.J. and Steitz,J.A. (2013) The 'Observer Effect' in genome-wide surveys of protein-RNA interactions. *Mol. Cell*, **49**, 601–604.

Rose,G.D. *et al.* (1985) Hydrophobicity of amino acid residues in globular proteins. *Science*, **229**, 834–838.

Rost,B. (1996) PHD: Predicting one-dimensional protein structure by profile-based neural networks. *Methods Enzymol.*, **266**, 525–539.

Shazman,S. and Mandel-Gutfreund,Y. (2008) Classifying RNA-binding proteins based on electrostatic properties. *PLoS Comput. Biol.*, **4**, e1000146.

Sickmeier,M. *et al.* (2007) DisProt: the database of disordered proteins. *Nucleic Acids Res.*, **35**, D786–D793.

Smialowski,P. *et al.* (2012) PROSO II—a new method for protein solubility prediction. *FEBS J.*, **279**, 2192–2200.

Smialowski,P. *et al.* (2010) The Negatome database: a reference set of non-interacting protein pairs. *Nucleic Acids Res.*, **38**, D540–D544.

Sweet,R.M. and Eisenberg,D. (1983) Correlation of sequence hydrophobicities measures similarity in three-dimensional protein structure. *J. Mol. Biol*, **171**, 479–488.

Tartaglia,G.G. *et al.* (2005) Organism complexity anti-correlates with proteomic beta-aggregation propensity. *Protein Sci.*, **14**, 2735–2740.

Tartaglia,G.G. *et al.* (2010) Physicochemical determinants of chaperone requirements. *J. Mol. Biol*, **400**, 579–588.

Tartaglia,G.G. *et al.* (2008) Prediction of aggregation-prone regions in structured proteins. *J. Mol. Biol.*, **380**, 425–436.

Tartaglia,G.G. *et al.* (2004) The role of aromaticity, exposed surface, and dipole moment in determining protein aggregation rates. *Protein Sci.*, **13**, 1939–1941.

Tartaglia,G.G. and Vendruscolo,M. (2010) Proteome-level interplay between folding and aggregation propensities of proteins. *J. Mol. Biol.*, **402**, 919–928.

Tartaglia,G.G. and Vendruscolo,M. (2008) The Zyggregator method for predicting protein aggregation propensities. *Chem. Soc. Rev.*, **37**, 1395–1401.

Terribilini,M. *et al.* (2006) Prediction of RNA binding sites in proteins from amino acid sequence. *RNA*, **12**, 1450–1462.

Wang,M. *et al.* (2012) PaxDb, a database of protein abundance averages across all three domains of life. *Mol. Cell Proteom.*, **11**, 492–500

Wertz,D.H. and Scheraga,H.A. (1978) Influence of water on protein structure. An analysis of the preferences of amino acid residues for the inside or outside and for specific conformations in a protein molecule. *Macromolecules*, **11**, 9–15.

Wilkins,M.R. *et al.* (1999) Protein identification and analysis tools in the ExPASy server. *Methods Mol. Biol.*, **112**, 531–552.

Wolpert,D.H. (2002) The supervised learning no-free-lunch theorems. In: *Soft Computing and Industry*. Springer, London, pp. 25–42.

Zanzoni,A. *et al.* (2013) Principles of self-organization in biological pathways: a hypothesis on the autogenous association of alpha-synuclein. *Nucleic Acids Res.*, **41**, 9987–9998

Zimmer,C. *et al.* (2001) Analysis of sequence-specific binding of RNA to Hsp70 and its various homologs indicates the involvement of N- and C-terminal interactions. *RNA*, **7**, 1628–1637.